

Tight-binding Central Interaction Model for the Band Structure of Silicon*

G. P. Betteridge

Physics and Engineering Laboratory,
Department of Scientific and Industrial Research,
Private Bag, Lower Hutt, New Zealand.

Abstract

We consider a simple tight-binding model involving all interactions between first and second nearest-neighbour (n.n.) bonds in the diamond lattice. We show that the band structure may be solved analytically in the central approximation in which all second n.n. bond interactions of the same type, for example all bonding : bonding or all bonding : antibonding interactions, are considered equal. The k dependence of the solution is given in terms of the corresponding s-band eigenvalues, which are determined by the topology of the structure. The model solution is compared with the results of a pseudopotential calculation for silicon. The tight-binding parameters are obtained by fitting to the pseudopotential energies at Γ and X , where the central solution is exact. The effects on the band structure of including second n.n. bond interactions, and interactions between bonding and antibonding states, are discussed. The complete solution provides a very good representation of both valence and conduction bands along ΓX , as well as an excellent fit to the lowest valence band throughout the zone. Comparison of the central solution with the pseudopotential bands away from ΓX clearly shows the effects of the angular-dependent non-central interactions omitted from the theory.

1. Introduction

Much of the appeal of tight-binding schemes for deriving electronic energy levels in solids is that they are based on a real-space picture of the intersite electronic interactions. These interactions may be resolved into a central component, which depends on the radial separation of the sites only, and a non-central component which depends on the angular relationship of the sites as well. The simplest example of a purely central system occurs for interactions between spherically symmetric s electrons. The resulting eigenvalues are determined by the topology of the structure only, and can normally be expressed in analytical form. In contrast, for systems containing higher momentum states (p, d, ...), the tight-binding interaction matrix contains both central and non-central contributions, and is generally so complex that an analytical solution is not feasible. In the case of sp^3 bonded silicon, the bonds have a pronounced directional character and we expect the non-central interactions to play an important role in determining features of the band structure. One way to study the relative importance of central and non-central contributions in such cases is to evaluate the band structure for just the central component and then compare this with the complete

* Paper presented at the Australia–New Zealand Condensed Matter Physics Meeting, Pakatoa Island, N.Z., 8–10 February 1984.

solution. This, we find, has the additional bonus that it results in a substantial simplification of the problem, to the extent that the solution may be obtained analytically in a manner very similar to the s-band case.

In this paper we derive an analytical solution of the tight-binding sp^3 band structure of silicon for central interactions only. The solution provides a direct connection between the local environment of the state and its energy. Furthermore, by comparison of the central solution with the results of a pseudopotential calculation, we establish the effects of the non-central interactions omitted from the theory.

The tight-binding scheme used here includes all central interactions between nearest-neighbour (n.n.) and second n.n. bonds, where the bonds are formed from bonding (b) and antibonding (a) combinations of sp^3 orbitals on neighbouring sites. In this way, we include all central interactions between sp^3 orbitals on the n.n. and second n.n. sites, as well as some third n.n. site interactions. These interactions are expected to give a good representation of the contribution of central interactions, since similar models which include non-central interactions give a good account of the complete band structure (Chadi and Cohen 1975; Tanaka and Tsu 1981).

This interaction model is an extension of one used earlier to study the effects of topological disorder in sp^3 bonded structures (Weaire 1971; Weaire and Thorpe 1971). This simpler model, which only considers interactions between sp^3 orbitals on the same site, or forming the same bond, allows a general analytical solution for the sp^3 band structure in terms of the s-band eigenvalues of the structure (Thorpe and Weaire 1971). This result has been rederived in several illuminating ways (Straley 1972; Schwartz and Ehrenreich 1972; Huang and Dy 1974), and in some cases for extended interaction models (Heine 1971; Hulin 1972; Weaire and Thorpe 1973; Streitwolf 1974; Lohez *et al.* 1981). In each case, however, the interactions have been confined to n.n. sites and are central, i.e. no angular-dependent terms have been included. As we will show, it is the central nature of these models which allows the reduction of the solution to analytical form. Conversely, many of the intriguing results obtained with these simple models (see e.g. Weaire and Thorpe 1973), also hold for more complex systems provided only central interactions are included.

The mathematical details of the central solution are given in Section 2. The s band is treated first, since its solution forms the basis of that for the sp^3 bands. The approach to the sp^3 solution adopted here follows Heine (1971) and Hulin (1972). As a first approximation we assume that there is no interaction between the bonding and antibonding states. Thus the interactions among the bonding states determine the valence band, while those among the antibonding states give the conduction band. These independent solutions are then used to determine the bonding-antibonding interaction matrix elements. This process is applied first to the n.n. bond interactions only, and then the second n.n. bond interactions are included. The effect of each of these interactions on the band structure is discussed in Section 3, where a comparison is made with the results of a local pseudopotential calculation for silicon. We conclude in the Appendix by outlining the fitting procedure used to obtain the tight-binding parameters for the model solution.

2. Mathematical Analysis

(a) The s Band

The s-band eigenvalues and eigenfunctions play a major role in the central interaction approximation for the sp^3 bands. We therefore begin by considering the

s-band structure of the diamond structure. This consists of two interpenetrating face-centred-cubic lattices, denoted by i and j , arranged so that the nearest neighbours of i all lie on j and vice versa. The unit cell contains two sites (one on each lattice) and we consider n.n. interactions between single s states on each site. The basis states can be formed from Bloch sums on each lattice:

$$|\phi_1\rangle = \sum_i \exp(i\mathbf{k}\cdot\mathbf{r}_i) |\phi_i\rangle, \quad |\phi_2\rangle = \sum_j \exp(i\mathbf{k}\cdot\mathbf{r}_j) |\phi_j\rangle. \quad (1a, b)$$

The solution of the secular equations is given by

$$\begin{vmatrix} -\varepsilon_s & \varepsilon \exp(i\theta) \\ \varepsilon \exp(-i\theta) & -\varepsilon_s \end{vmatrix} = 0, \quad (2)$$

where ε_s is the required eigenvalue, and

$$\varepsilon \exp(i\theta) = V \sum_{j'} \exp\{i\mathbf{k}\cdot(\mathbf{r}_{j'} - \mathbf{r}_i)\}. \quad (3)$$

The prime on the summation indicates that the sum is to be taken over the four nearest neighbours, j' , of i . The magnitude of the n.n. interaction V will be taken as unity or, equivalently, ε_s is measured in units of V .

The solution of equation (2) is

$$\varepsilon_s = \pm \varepsilon, \quad (4)$$

where for the diamond structure (Weaire and Thorpe 1971)

$$\varepsilon = 2(1 + \alpha_{xyz})^{\frac{1}{2}}, \quad (5a)$$

with

$$\alpha_{xyz} = \cos \pi k_x \cos \pi k_y + \cos \pi k_y \cos \pi k_z + \cos \pi k_z \cos \pi k_x. \quad (5b)$$

Note from equation (4) that, since ε is real,

$$\sum_j \cos\{\mathbf{k}\cdot(\mathbf{r}_j - \mathbf{r}_i) - \theta\} = \varepsilon, \quad \sum_j \sin\{\mathbf{k}\cdot(\mathbf{r}_j - \mathbf{r}_i) - \theta\} = 0. \quad (6a, b)$$

The eigenfunctions corresponding to $\pm \varepsilon$ may be written as

$$\sqrt{2}\psi_{\pm}(\mathbf{k}) = |\phi_1\rangle \pm \exp(-i\theta) |\phi_2\rangle, \quad (7)$$

so that from equations (1) the site coefficients are

$$C_i^{\pm} = \exp(i\mathbf{k}\cdot\mathbf{r}_i), \quad C_j^{\pm} = \pm \exp(-i\theta) \exp(i\mathbf{k}\cdot\mathbf{r}_j). \quad (8a, b)$$

Using equation (3), we find

$$\sum_i C_i^{\pm} = \pm \varepsilon C_j^{\pm}, \quad \sum_j C_j^{\pm} = \pm \varepsilon C_i^{\pm}. \quad (9a, b)$$

Thus, for an eigenstate of a central interaction matrix, the product of the eigenvalue and the amplitude of the eigenfunction on any site equals the sum of the amplitudes on the n.n. sites. These relationships (equations 9) are of considerable importance in obtaining the correct central solution for the sp^3 bands. As noted by Weaire

and Thorpe (1973), they are the basis of the one-band-two-band transformation used by them to express the sp^3 eigenvalues in terms of the s -band solutions ϵ .

(b) The sp^3 Bands

To represent silicon in the diamond lattice we need to replace the single s state per atom discussed in the previous subsection by four sp^3 hybridized orbitals. Each of these orbitals is oriented along one of the four tetrahedral directions linking n.n. sites. The two sp^3 orbitals which point towards each other from n.n. i and j sites may be combined together to form a bond. This can be achieved in two ways; either with the same phase forming a bonding orbital $|B, ij\rangle$, or with opposite phase forming an antibonding orbital $|A, ij\rangle$. Thus, if $|uv\rangle$ is an sp^3 orbital on site u pointing towards site v , we have

$$\sqrt{2}|B, ij\rangle = |ij\rangle + |ji\rangle, \quad \sqrt{2}|A, ij\rangle = |ij\rangle - |ji\rangle. \quad (10a, b)$$

These orbitals are defined on the i lattice only. This avoids normalization problems which arise if the orbits are defined on both lattices (Heine 1971). Thus we always consider $|B, ji\rangle$ equivalent to $|B, ij\rangle$ and similarly for $|A, ji\rangle$ and $|A, ij\rangle$. This convention also uniquely defines the phase of $|A, ij\rangle$; the positive sp^3 orbital is always on site i , as in equations (10).

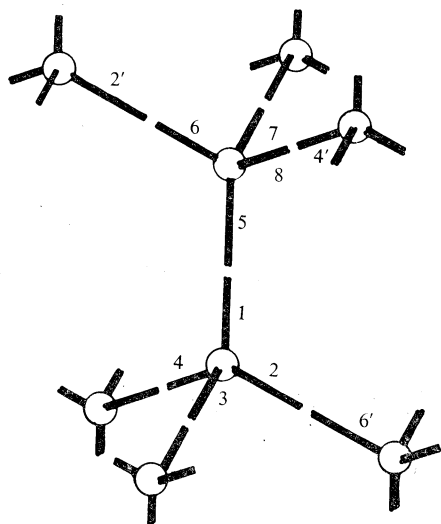


Fig. 1. Section of the diamond lattice showing the four sp^3 orbitals on each site. Interactions between these orbitals are defined in Table 1.

Table 1. Notation used for (a) the interaction matrix elements between sp^3 orbitals (see Fig. 1) and (b) the expansion of first and second n.n. bond interactions in terms of the sp^3 interactions (see Section 2b)

| (a) sp^3 orbitals | | | | (b) Bonds | | | |
|------------------------|-------|--------------------------|----------|-------------|-------------------|----------------|--------------------|
| $\langle 1 H 2\rangle$ | V_1 | $\langle 1 H 4'\rangle$ | V_7 | v_0^b | V_2 | v_0^a | $-V_2$ |
| $\langle 1 H 5\rangle$ | V_2 | $\langle 2 H 2'\rangle$ | V_8 | $2v_1^b$ | $V_1+2V_3+V_7$ | $2v_1^a$ | $V_1-2V_3+V_7$ |
| $\langle 2 H 5\rangle$ | V_3 | $\langle 2 H 4'\rangle$ | V_9 | $2v_{2c}^b$ | $V_5+2V_9+V_{11}$ | $2v_{2c}^a$ | $-V_5+2V_9-V_{11}$ |
| $\langle 2 H 6\rangle$ | V_4 | $\langle 4' H 6'\rangle$ | V_{11} | $2v_{2t}^b$ | $V_4+2V_8+V_{12}$ | $2v_{2t}^a$ | $-V_4+2V_8-V_{12}$ |
| $\langle 2 H 8\rangle$ | V_5 | $\langle 2' H 6'\rangle$ | V_{12} | $2v_1^{ab}$ | V_5-V_{11} | $2v_{2t}^{ab}$ | V_4-V_{12} |
| | | | | $2v_1^{ab}$ | V_1-V_7 | | |

A section of the diamond lattice is shown schematically in Fig. 1. The notation used here for the interaction matrix elements between sp^3 orbitals follows Tanaka and Tsu (1981) and is given in Table 1a. Note that their V_6 and V_{10} correspond to third n.n. bond interactions and are excluded here, while we have included the second n.n. bond interaction V_{12} . Interactions between the various bonding and antibonding states may be expressed in terms of these interactions using equations (10); these are given in Table 1b. A subscript 1 or 2 is used to denote first or second n.n. bond interactions respectively, and a superscript b, a, or ab denotes bonding–bonding, antibonding–antibonding and bonding–antibonding interactions respectively. The additional subscript c or t on the second n.n. bond interactions corresponds to the two possible orientations ('cis' and 'trans') of these bonds in the diamond structure.

We have also included v_0^b and v_0^a which correspond to the 'self-energies' of the bonding and antibonding states. These correspond to the sp^3 interactions V_2 and $-V_2$ respectively. In the normal situation we have $V_2 < 0$ so that the bonding states have lower energy than the antibonding states.

As mentioned in the Introduction, we initially consider the valence band to be formed by interactions among the bonding states only, and the conduction band from interactions among the antibonding states only. These solutions are then used to incorporate the bonding–antibonding interaction.

Nearest-neighbour bonding interactions. To determine the eigenvalues of the central bonding sub-matrix, we follow a scheme used by Weaire and Thorpe (1973) and developed by Joannopoulos and Cohen (1976). We begin by forming a trial wavefunction $|B\rangle$ from a linear superposition of the bonding states:

$$|B\rangle = \sum_i \left(\sum_{j'} b_{ij'} |B, ij'\rangle \right), \quad (11)$$

where again the prime on the summation indicates that the sum is taken over the four j' nearest neighbours of i only. Note that since there are four orbitals at each site, the bonding sub-matrix is 4×4 and will have four solutions.

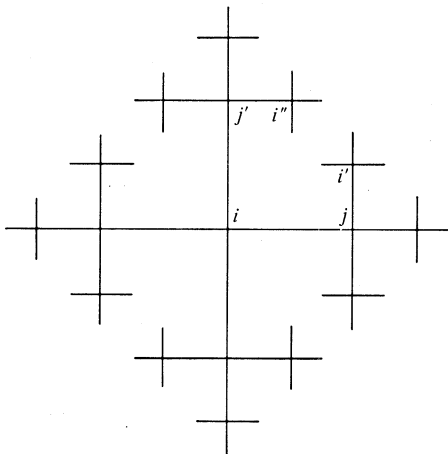


Fig. 2. Schematic diagram showing the connectivity of the diamond lattice out to all second n.n. bonds about the site i .

The central solution for $|B\rangle$ may be obtained by analogy with the s-band solution, but first we must re-examine what we mean by the central approximation. It may

be stated as the requirement that the interactions between all equidistant pairs of sites must be equal. This is automatically satisfied in the s-band case, and results in the eigenfunction satisfying equations (9). In the sp^3 case however there are four orbitals at each lattice site. The corresponding approximation for sp^3 states is, therefore, that the total interaction of all four bonds at site i , with all four bonds at site j , must be the same for all equidistant pairs of sites. This condition is readily satisfied if all m th n.n. bond interactions are taken to be equal. Then, by analogy with the s-band solution, the central solution for $|B\rangle$ is given by equations (9) with the individual amplitudes replaced by $\sum_{j'} b_{ij'}$. Note that requiring all m th n.n. bond interactions to be equal is strictly equivalent to ignoring angular variations, as we see when discussing second n.n. bond interactions in the following subsection.

Referring to Fig. 1, we see that all n.n. bonds in the diamond lattice have the same relative orientation and therefore the same interaction, denoted by v_1^b . Thus the n.n. bonding solution is purely central in character. Inserting the trial eigenfunction into Schrödinger's equation, we find for all bonds $|B, ij\rangle$ that

$$(E^b - v_0^b)b_{ij} = v_1^b \left(\sum_{j'} b_{ij'} - b_{ij} + \sum_{i'} b_{i'j} - b_{ij} \right). \quad (12)$$

(We adopt a notation whereby j' represents nearest neighbours of i , i' nearest neighbours of j , j'' nearest neighbours of i' , and so on; see Fig. 2.) In equation (12), E^b is the required bonding eigenvalue. The right-hand side has been expanded to show how the sums over all coefficients at each site may be formed by adding and subtracting the missing coefficients. The notation is simplified by writing

$$b_i = \sum_{m'} b_{im'}, \quad (13)$$

so that equation (12) becomes

$$(E^b - v_0^b + 2v_1^b)b_{ij} = v_1^b(b_i + b_j). \quad (14)$$

There are similar equations for each bond, so that by summing over j' we have

$$(E^b - v_0^b + 2v_1^b)b_i = v_1^b \left(4b_i + \sum_j b_j \right). \quad (15)$$

However, for a central solution we know that the sum over b_j must satisfy equations (9), i.e. $\sum_j b_j$ is equal to $\pm \epsilon b_i$, and thus the central solution is given by

$$(E^b - v_0^b + 2v_1^b)b_i = v_1^b(4 \pm \epsilon)b_i,$$

that is,

$$E_{\pm}^b = v_0^b + (2 \pm \epsilon)v_1^b. \quad (16)$$

We refer to these two solutions as the sp bands, since at Γ ($\mathbf{k} = 0$) they correspond to states of pure s (E_+^b) and pure p (E_-^b) character (Weaire and Thorpe 1971).

The remaining two solutions are pure p states for which $b_i = b_j = 0$ (Hulin 1972). They are degenerate with energy given from equation (14) as

$$E_{\pi}^b = v_0^b - 2v_1^b. \quad (17)$$

We refer to these as π bands. These solutions were first derived by Weaire and Thorpe (1971) with v_1^b given by V_1 .

The present method has the added advantage that the eigenfunctions corresponding to E_{\pm}^b can be readily obtained. Substituting for E_{\pm}^b into equation (14), we see that the corresponding coefficients b_{ij}^{\pm} must obey

$$(4 \pm \varepsilon)b_{ij}^{\pm} = b_i^{\pm} + b_j^{\pm}. \quad (18)$$

This is satisfied by (see equations 9)

$$N_{\pm} b_{ij}^{\pm} = C_i^{\pm} + C_j^{\pm}, \quad (19)$$

where N_{\pm} is the normalization factor

$$\begin{aligned} N_{\pm}^2 &= \sum_i \sum_j' (C_i^{\pm} + C_j^{\pm})^* (C_i^{\pm} + C_j^{\pm}) \\ &= \sum_i \sum_j' [2 \pm 2 \cos\{\mathbf{k} \cdot (\mathbf{r}_j - \mathbf{r}_i) - \theta\}] \\ &= (4 \pm \varepsilon)N, \end{aligned} \quad (20)$$

and where we have used equations (8) and (6). Here N is the total number of sites in the diamond lattice (i.e. twice the number of i -lattice sites). Thus, we have

$$b_{ij}^{\pm} = (4 \pm \varepsilon)^{-\frac{1}{2}} N^{-\frac{1}{2}} \exp(i\mathbf{k} \cdot \mathbf{r}_i) [1 \pm \exp(-i\theta) \exp\{i\mathbf{k} \cdot (\mathbf{r}_j - \mathbf{r}_i)\}]. \quad (21)$$

Note that these states are also orthogonal since, by equation (6b),

$$\begin{aligned} \sum_i \sum_j' (b_{ij}^{\pm})^* b_{ij}^{\mp} &= (16 - \varepsilon^2)^{-\frac{1}{2}} N^{-1} \sum_i \sum_j' 2i \sin\{\mathbf{k} \cdot (\mathbf{r}_j - \mathbf{r}_i) - \theta\} \\ &= 0. \end{aligned} \quad (22)$$

Second n.n. bonding interactions. Unlike the situation for n.n. bonds, the second n.n. bond interactions in the diamond structure are not all equivalent (see Fig. 1). The magnitude of the interaction depends on the relative orientation of the bonds as determined by the dihedral angle (i.e. the angle between the two bonds as projected onto a plane normal to the common axis between the sites). It can be shown quite generally that $v_2(\phi)$ has the form (Betteridge 1974)

$$v_2(\phi) = a + b \cos \phi, \quad (23)$$

where a and b are constants. Thus for a central model it would be quite appropriate to set all v_2 equal to a . However, for the diamond structure it is more convenient to select an alternative value for v_2 . (Note that the central approximation is satisfied for any constant value of v_2 .)

Consider the relative orientations of a bond at i , say $|B, ij\rangle$, with the three second n.n. bonds which meet at j' ($\neq j$) (see Figs 1 and 2). One of these bonds is parallel to, and indeed translationally equivalent to, $|B, ij\rangle$. We refer to this as the trans-orientation, for which $\phi = \pi$, and the interaction is denoted by v_{2t}^b . The other two

bonds are symmetrically placed on either side of $|B, ij\rangle$, with $\phi = \pm \frac{1}{2}\pi$. We refer to these as cis-orientations and the interaction, denoted by v_{2c}^b , is the same in each case. The same situation occurs for each of the six vertices (j' or i') at which second n.n. bonds to $|B, ij\rangle$ meet. Thus each bond has eighteen second n.n. bonds, twelve of which are in the cis-orientation and six in the trans-orientation. We therefore choose to treat all second n.n. bond interactions as though they were in the cis-orientation, i.e. $v_2(\phi)$ is taken as v_{2c}^b . Thus, the only approximation involves the trans-oriented bonds. We consider these in more detail later in Section 2e.

We can now evaluate the second n.n. bond contribution by the same technique used for the nearest neighbours (see Fig. 2):

$$(E_{\pm}^b - E_{nn}^b)b_{ij}^{\pm} = v_{2c}^b \left(\sum_{j'} b_{j'} - b_i - b_j + b_{ij} + \sum_{i'} b_{i'} - b_j - b_i + b_{ij} \right), \quad (24)$$

where E_{nn}^b is the n.n. solution given by equation (16). Using equations (9) and (18), we have

$$(E_{\pm}^b - E_{nn}^b - 2v_{2c}^b)b_{ij}^{\pm} = v_{2c}^b(-2 \pm \epsilon)(4 \pm \epsilon)b_{ij}^{\pm},$$

that is,

$$E_{\pm}^b = v_0^b + (2 \pm \epsilon)v_1^b + (\epsilon^2 \pm 2\epsilon - 6)v_{2c}^b. \quad (25)$$

Similarly, putting $b_i = b_j = 0$ in equation (24) yields

$$E_{\pi}^b = v_0^b - 2v_1^b + 2v_{2c}^b \quad (\text{two-fold degenerate}). \quad (26)$$

(c) Antibonding Interactions

The solutions for the antibonding bands may be constructed by analogy with the bonding solution. The antibonding eigenfunctions are

$$|A\rangle = \sum_i \sum_{j'} a_{ij'} |A, ij'\rangle. \quad (27)$$

With our sign convention for the $|A, ij\rangle$, i.e. the positive orbital is at the i site, all n.n. interactions between antibonding states take the same value v_1^a , as do all second n.n. bond interactions in the cis- (v_{2c}^a) or trans- (v_{2t}^a) orientations. The secular equations are therefore of precisely the same form as for the bonding states, with all b 's (superscripts and coefficients) replaced by a 's. We therefore have

$$E_{\pm}^a = v_0^a + (2 \pm \epsilon)v_1^a + (\epsilon^2 \pm 2\epsilon - 6)v_{2c}^a, \quad (28)$$

$$E_{\pi}^a = v_0^a - 2v_1^a + 2v_{2c}^a \quad (\text{two-fold degenerate}), \quad (29)$$

and $a_{ij}^{\pm} = b_{ij}^{\pm}$.

From the orthogonality relationships for the b_{ij} (equation 22), we have

$$\sum_i \sum_{j'} (a_{ij'}^{\pm})^* a_{ij'}^{\pm} = 1 = \sum_i \sum_{j'} (a_{ij'}^{\pm})^* b_{ij'}^{\pm}, \quad (30a)$$

$$\sum_i \sum_{j'} (a_{ij'}^{\pm})^* a_{ij'}^{\mp} = 0 = \sum_i \sum_{j'} (a_{ij'}^{\pm})^* b_{ij'}^{\mp}. \quad (30b)$$

(d) Bonding–Antibonding Interactions

Having established the eigenvalues and eigenfunctions of the bonding and antibonding sub-bands, we now consider the interactions between them. In particular, we concentrate on the interactions between the sp bands only.

Nearest-neighbour interactions. We define the n.n. bonding–antibonding interaction as that between a bonding and an antibonding state both centred at i :

$$v_1^{ab} = \langle A, ij' | H_1^{ab} | B, ij \rangle. \quad (31)$$

Due to our sign convention for $|A, ij\rangle$, the other possibility, in which the two states meet at j , has opposite sign, i.e.

$$-v_1^{ab} = \langle A, i'j | H_1^{ab} | B, ij \rangle. \quad (32)$$

Thus, for each bond $|B, ij\rangle$, we have

$$H_1^{ab} | B, ij \rangle = v_1^{ab} \left(\sum_j' | A, ij' \rangle - | A, ij \rangle - \sum_i' | A, i'j \rangle + | A, ij \rangle \right), \quad (33)$$

so that in forming the matrix element with $|A\rangle$, each b_{ij} will be multiplied by a factor $(a_i - a_j)^*$ which, by equations (9), gives

$$(a_i^\pm - a_j^\pm)^* = (4 \pm \varepsilon)(a_{ij}^\mp)^* N_\mp / N_\pm, \quad (34)$$

where we note the change in the order of the signs in the superscript on a_{ij} . From the orthogonality relationships (30), the only nonzero matrix elements are

$$\langle A^\mp | H_1^{ab} | B^\pm \rangle = (16 - \varepsilon^2)^{\frac{1}{2}} v_1^{ab}. \quad (35)$$

Second n.n. interactions. The second n.n. bonding–antibonding interaction is defined as

$$v_2^{ab} = -\langle A, i''j' | H_2^{ab} | B, ij \rangle, \quad (36)$$

i.e. the interacting states are separated by a bond at i . The other possibility in which the bonds are separated by a bond at j has the opposite sign. Again there are two orientations, cis and trans, and as in the previous cases we treat all the interactions as if cis-oriented. From Fig. 2, we have

$$\begin{aligned} H_2^{ab} | B, ij \rangle &= -v_{2c}^{ab} \left[\sum_j' \left(\sum_{i''} | A, i''j' \rangle - | A, ij' \rangle \right) - \sum_i' | A, i'j \rangle + | A, ij \rangle \right. \\ &\quad \left. - \left\{ \sum_{i'}' \left(\sum_{j''} | A, i'j'' \rangle - | A, i'j \rangle \right) - \sum_{j'}' | A, ij' \rangle + | A, ij \rangle \right\} \right] \\ &= -v_{2c}^{ab} \left(\sum_j' \sum_{i''} | A, i''j' \rangle - \sum_{i'}' \sum_{j''} | A, i'j'' \rangle \right). \end{aligned} \quad (37)$$

The matrix element now involves

$$-v_{2c}^{ab} \sum_i' \sum_{j'}' b_{ij'} \left(\sum_{j''} a_{j''}^* - \sum_{i''} a_{i''}^* \right) = \mp v_{2c}^{ab} \sum_i' \sum_{j'}' b_{ij'} \varepsilon (4 \pm \varepsilon) (a_{ij}^\mp)^* N_\mp / N_\pm. \quad (38)$$

Therefore the total nonzero matrix elements are

$$\langle A^\mp | H^{ab} | B^\pm \rangle = (16 - \varepsilon^2)^{\frac{1}{2}} (v_1^{ab} \pm \varepsilon v_{2c}^{ab}) = V_\pm^{ab}. \quad (39)$$

The bonding–antibonding interaction couples the states in pairs, the eigenvalues being given by the solutions of

$$\begin{vmatrix} E_{\pm}^b - E & V_{\pm}^{ab} \\ V_{\pm}^{ab} & E_{\mp}^a - E \end{vmatrix} = 0,$$

that is,

$$E = E_{\pm}^b + E_{\mp}^a \pm \{(E_{\pm}^b - E_{\mp}^a)^2 + (V_{\pm}^{ab})^2\}^{\frac{1}{2}}, \quad (40)$$

together with the π states given by equations (26) and (29).

(e) *Trans-interactions*

The only approximation made so far concerns the treatment of the trans-oriented states. We now show that some corrections to these interactions can still be made within the central approximation.

The trans-oriented bonds are all related to one another by translations of the lattice; for example, if $|B, i''j'\rangle$ and $|B, ij\rangle$ are such a pair, we have

$$|B, i''j'\rangle = \exp\{i\mathbf{k} \cdot (\mathbf{r}_i - \mathbf{r}_{i''})\} |B, ij\rangle. \quad (41)$$

The interactions between these states are therefore diagonal in the $|B, ij\rangle$ basis. Thus, using the orbitals oriented along $(1\bar{1}\bar{1})$ as an example, we find for the bonding–bonding interaction

$$\begin{aligned} H_t^b |B, 1\bar{1}\bar{1}\rangle &= (v_{2t}^b - v_{2c}^b) \{2 \cos \pi(k_x - k_y) + 2 \cos \pi(k_y + k_z) \\ &\quad + 2 \cos \pi(k_z - k_x)\} |B, 1\bar{1}\bar{1}\rangle \\ &= (v_{2t}^b - v_{2c}^b) (2\alpha_{xyz} + 2 \sin \pi k_x \sin \pi k_y - 2 \sin \pi k_y \sin \pi k_z \\ &\quad + 2 \sin \pi k_z \sin \pi k_x) |B, 1\bar{1}\bar{1}\rangle, \end{aligned} \quad (42)$$

with similar terms for the other bonds. The magnitude of the interaction is taken as $v_{2t}^b - v_{2c}^b$ since these interactions have already been included with amplitude v_{2c}^b . The sign of the sine terms in equation (42) depends on the orientation of the bond, so that the total interaction is beyond the central approximation. However, the $2\alpha_{xyz}$ contribution is common to all bonds, so that within the spirit of the central interaction we may take

$$\begin{aligned} H_t^b |B, ij\rangle &= 2\alpha_{xyz} (v_{2t}^b - v_{2c}^b) |B, ij\rangle \\ &= (\frac{1}{2}\varepsilon^2 - 2)(v_{2t}^b - v_{2c}^b) |B, ij\rangle, \end{aligned} \quad (43)$$

by equation (5a). This contribution occurs for all $|B, ij\rangle$, and can therefore be simply added to our previous solutions. An analogous argument holds for the antibonding bands, so that we now have

$$E_{\pm}^b = v_0^b + (2 \pm \varepsilon)v_1^b + (\frac{1}{2}\varepsilon^2 \pm 2\varepsilon - 4)v_{2c}^b + (\frac{1}{2}\varepsilon^2 - 2)v_{2t}^b, \quad (44a)$$

$$E_{\pm}^a = v_0^a + (2 \pm \varepsilon)v_1^a + (\frac{1}{2}\varepsilon^2 \pm 2\varepsilon - 4)v_{2c}^a + (\frac{1}{2}\varepsilon^2 - 2)v_{2t}^a, \quad (44b)$$

$$E_{\pi}^b = v_0^b - 2v_1^b + (4 - \frac{1}{2}\varepsilon^2)v_{2c}^b + (\frac{1}{2}\varepsilon^2 - 2)v_{2t}^b, \quad (44c)$$

$$E_{\pi}^a = v_0^a - 2v_1^a + (4 - \frac{1}{2}\varepsilon^2)v_{2c}^a + (\frac{1}{2}\varepsilon^2 - 2)v_{2t}^a. \quad (44d)$$

We note from (42), that all the sine terms vanish along ΓX [$\mathbf{k} = 2\pi(k, 0, 0)/a$]. Therefore equations (44) are exact solutions along ΓX in the absence of the bonding-antibonding interaction.

The trans-contribution to the bonding-antibonding matrix element can be calculated in a similar manner; for example,

$$H_{\pm}^{\text{ab}} | \text{B}, 1\bar{1}\bar{1} \rangle = i(v_{2\text{t}}^{\text{ab}} - v_{2\text{c}}^{\text{ab}}) \{ 2 \sin \pi(k_y + k_z) - 2 \sin \pi(k_x - k_y) + 2 \sin \pi(k_z - k_x) \} | \text{A}, 1\bar{1}\bar{1} \rangle, \quad (45)$$

with similar expressions for the other directions. In this case all the signs depend on the direction of the bond and there is no common contribution. However, it is of interest to evaluate the interaction along ΓX ; in this case both (111) and (1 $\bar{1}\bar{1}$) bonds yield $-4i \sin \pi k(v_{2\text{t}}^{\text{ab}} - v_{2\text{c}}^{\text{ab}})$, while (1 $\bar{1}\bar{1}$) and (11 $\bar{1}$) yield $4i \sin \pi k(v_{2\text{t}}^{\text{ab}} - v_{2\text{c}}^{\text{ab}})$. Also, from equation (3), and by writing $\frac{1}{2}\pi k_x = \xi_x$, we have $\varepsilon \exp(i\theta) = 4 \cos \xi_x$, i.e.

$$\theta = 0, \quad (46a)$$

$$b_{ij}^{\pm} = \exp(i\mathbf{k} \cdot \mathbf{r}_i) [1 \pm \exp\{(\pm)i\xi_x\}] / N_{\pm}, \quad (46b)$$

where (\pm) is positive for (111) and (1 $\bar{1}\bar{1}$), and negative for (1 $\bar{1}\bar{1}$) and (11 $\bar{1}$) directed bonds. Combining these results, the trans-contribution to the nonzero matrix elements is

$$\begin{aligned} \langle A^{\mp} | H_{\pm}^{\text{ab}} | B^{\pm} \rangle &= (16 - \varepsilon^2)^{-\frac{1}{2}} N^{-1} 4i \sin 2\xi_x (v_{2\text{t}}^{\text{ab}} - v_{2\text{c}}^{\text{ab}}) \\ &\quad \times \sum_i [2\{1 \mp \exp(i\xi_x)\}\{1 \pm \exp(-i\xi_x)\} \\ &\quad \quad - 2\{1 \mp \exp(-i\xi_x)\}\{1 \pm \exp(i\xi_x)\}] \\ &= \pm (16 - \varepsilon^2)^{-\frac{1}{2}} 16 \sin \xi_x \sin 2\xi_x (v_{2\text{t}}^{\text{ab}} - v_{2\text{c}}^{\text{ab}}). \end{aligned} \quad (47)$$

Note that the sum over i gives only $\frac{1}{2}N$ terms. However, from equations (46), we have (along ΓX) $4 \sin \xi_x = (16 - \varepsilon^2)^{\frac{1}{2}}$ and $8 \sin 2\xi_x = \varepsilon(16 - \varepsilon^2)^{\frac{1}{2}}$, so that finally

$$\langle A^{\mp} | H_{\pm}^{\text{ab}} | B^{\pm} \rangle = \pm \frac{1}{2} \varepsilon (16 - \varepsilon^2)^{\frac{1}{2}} (v_{2\text{t}}^{\text{ab}} - v_{2\text{c}}^{\text{ab}}). \quad (48)$$

Combining this with our earlier result gives an average interaction

$$V_{\pm}^{\text{ab}} = (16 - \varepsilon^2)^{\frac{1}{2}} \{ v_{\text{t}}^{\text{ab}} \pm \frac{1}{6} \varepsilon (v_{2\text{t}}^{\text{ab}} + 3v_{2\text{c}}^{\text{ab}}) \}. \quad (49)$$

This expression has the same functional dependence on \mathbf{k} as our earlier solution, but with a different amplitude. However, the choice of amplitude is somewhat arbitrary, the main point being that all bonds are treated equally. Thus equation (49), which should provide a good approximation along ΓX , is taken to be the central solution throughout the zone.

Our final solution therefore retains the form given by equation (40) but with values of E_{\pm} given by equations (44) and V_{\pm}^{ab} given by equation (49).

3. Discussion

The expressions derived above are exact for an interaction model incorporating central components of first and second n.n. bond interactions in the diamond structure. In particular, the \mathbf{k} dependence, which is determined entirely by the topology

through $\varepsilon(\mathbf{k})$, is physically correct for this approximation, as is the dependence on the interaction matrix elements (the v 's). As is normal in the application of the tight-binding method, we will not attempt to determine the v 's from first principles, but rather choose them empirically by comparison of the central solution with the bands obtained from a more complete calculation (i.e. one which includes the non-central contribution as well). For this purpose we have chosen the band structure of silicon, as given by a local empirical pseudopotential calculation (see e.g. Cohen and Bergstresser 1966).

The band structure in the central approximation obviously cannot give a full description of the bands throughout the Brillouin zone, unless of course the actual forces are purely central. For this reason it is absolutely necessary that the fitting only be attempted at points where the central solution is expected to provide an accurate representation. From the discussion of the trans-interactions in Section 2e, we expect the solution to be accurate at the Γ and X points, and indeed with the amended form of the bonding-antibonding matrix element (equation 49), along all ΓX . Fortunately the complete tight-binding Hamiltonian matrix, including the non-central interactions, can be solved analytically at these points (Slater and Koster 1954; Chadi and Cohen 1975; Tanaka and Tsu 1981). The central solution at Γ and X , expressed in terms of the V_i (Table 1), is indeed identical to the results obtained by Tanaka and Tsu (1981). (In other words, the solutions at these points involve only central interactions as noted in Section 2e.) We therefore use just these two points, Γ and X , and in the case of the complete solution, $\frac{1}{2}\Gamma X$, to obtain the parameters. In this way the differences between the central solution and the pseudopotential bands in other directions, e.g. ΓL and ΓK , should provide a realistic indication of the contribution of the non-central interactions.

The solutions as derived clearly show the relationship between the energies and the interbond interactions; however, these are not the most convenient form for fitting to the pseudopotential results. We note that all of the \mathbf{k} dependence is in ε , and that the pure bonding, antibonding and π solutions may be written quite generally in the form

$$E = c_0 \pm c_1\varepsilon + c_2\varepsilon^2. \quad (50)$$

The coefficients can be readily expressed in terms of the v 's by comparison with equations (44); for example, for the sp bonding solutions up to second nearest neighbours we have

$$c_0^b = v_0^b + 2v_1^b - 4v_{2c}^b - 2v_{2t}^b, \quad (51a)$$

$$c_1^b = v_1^b + 2v_{2c}^b, \quad c_2^b = \frac{1}{2}(v_{2c}^b + v_{2t}^b), \quad (51b, c)$$

and for the π -bonding states

$$c_0^{\pi b} = v_0^b - 2v_1^b + 4v_{2c}^b - 2v_{2t}^b, \quad (52a)$$

$$c_1^{\pi b} = 0, \quad c_2^{\pi b} = \frac{1}{2}(v_{2t}^b - v_{2c}^b). \quad (52b, c)$$

Similar expressions hold for the antibonding coefficients with a replacing the b superscripts.

Using the form given in equation (50) simplifies considerably the fitting procedure at Γ and X . At Γ , we have $\varepsilon = 4$, so that the bonding-antibonding terms, which

vary as $(16-\varepsilon^2)^{\frac{1}{2}}$, vanish. Hence the solutions at Γ are always given by the pure bonding and antibonding solutions. At X , we have $\varepsilon = 0$, so that the pure bonding and antibonding solutions involve the c_0 only, while the bonding-antibonding interaction is given by the n.n. term $4v_1^{ab}$ only. Details of the fitting procedure used in the following examples are given in the Appendix.

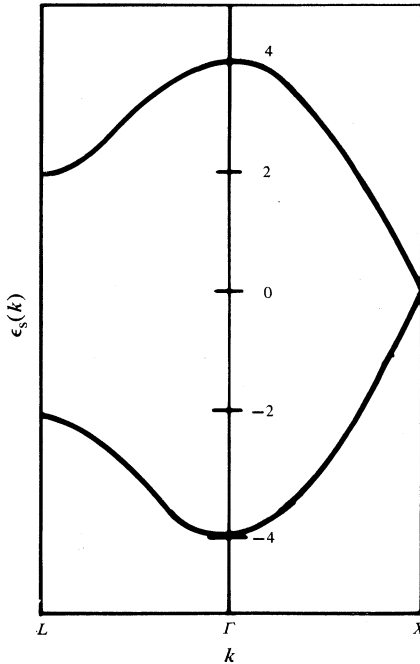


Fig. 3. The s-band structure for the diamond lattice along $\Gamma L [2\pi(k, k, k)/a]$ and $\Gamma X [2\pi(k, 0, 0)/a]$.

(a) The s Band

The s-band solution is given by $\pm \varepsilon(k)$ and is shown in Fig. 3. The main characteristics of this solution, which were also discussed by Chadi and Cohen (1975), are that it is symmetric about zero and has a pronounced rounded shape. The maximum splitting (bandwidth) occurs at Γ ($\varepsilon = 4$) while the bands are degenerate at X ($\varepsilon = 0$). At L ($\varepsilon = 2$), the bands are split symmetrically about zero [i.e. $E(X)$], with a separation equal to half the bandwidth at Γ .

(b) Nearest-neighbour Bonding and Antibonding Solutions

These solutions have the form

$$E_{\pm} = c_0 \pm c_1 \varepsilon, \quad E_{\pi} = c_0 - 4c_1 \quad (\text{doubly degenerate}), \quad (53a, b)$$

and are shown in Fig. 4a. The four parameters are uniquely defined by the energies at Γ . It is apparent from equations (53) that the sp solutions are equivalent to the s-band solution, now centred about c_0 and scaled by c_1 . Thus no matter how we choose c_0 and c_1 , the sp bands will retain all the characteristics of the s-band solution discussed above. The energy of the π bands is constant, a feature common to all n.n. bond solutions. We note in this respect that the Weaire-Thorpe (1971) model, and the extension of it discussed by Heine (1971), are all contained within this n.n. bond model.

For comparison, the pseudopotential bands are given in Fig. 4*b*. In contrast to the *s* bands, the pseudopotential bands are quite asymmetric, so that the bands at *X* are considerably lower than mid-band, and the second valence band in particular falls off steeply from Γ (i.e. it is not rounded as is the *s* band). Furthermore, the splitting at *L* is nearer to a quarter than half the bandwidth, and is not symmetrically placed about $E(X)$. The conduction band is quite different from that given by the central model.

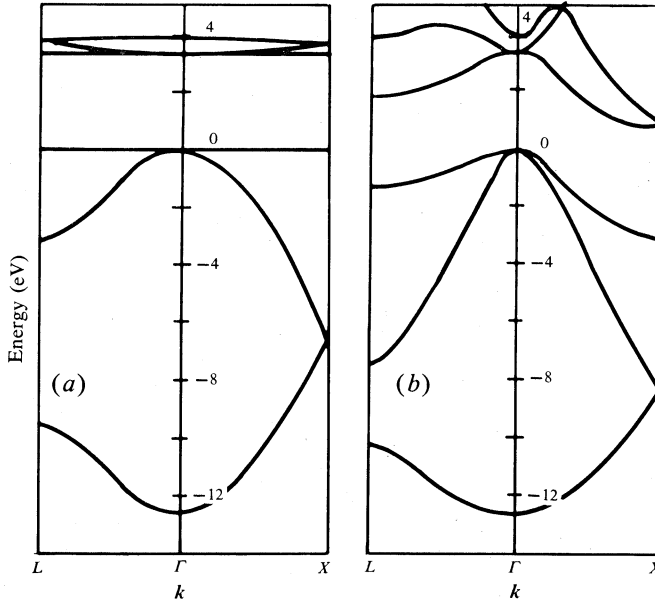


Fig. 4. Comparison of (a) the pure bonding and antibonding bands for n.n. bond interactions only, with (b) results of a pseudopotential calculation for silicon. Parameters used in (a) are (in eV): $c_0^b = -6.32$, $c_1^b = -1.58$, $c_0^{\pi b} = 0$, $c_0^a = 3.62$, $c_1^a = 0.06$ and $c_0^{\pi a} = 3.39$.

Thus the n.n. bond interaction model (without bonding–antibonding interactions) is totally inadequate as a model of even the sp^3 valence bands. In particular, we need to introduce terms which lead to some asymmetries in the bands.

(c) Nearest-neighbour Bonding–Antibonding Solution

The bonding–antibonding interaction couples the conduction and valence *sp* bands together in pairs. Indeed, by considering the nature of the states at Γ , we see that it couples *s*-like and *p*-like states. The form of the *sp* bands is

$$E_{sp} = \frac{1}{2}(c_0^b + c_0^a) \pm \varepsilon \frac{1}{2}(c_1^b - c_1^a) \\ (\pm) \left[\left\{ \frac{1}{2}(c_0^b - c_0^a) \pm \varepsilon \frac{1}{2}(c_1^b + c_1^a) \right\}^2 + (16 - \varepsilon^2)(v_1^{ab})^2 \right]^{\frac{1}{2}}, \quad (54)$$

where (\pm) indicates that both signs are taken independently of the other signs. Some asymmetry is introduced into the bands by the new term $(16 - \varepsilon^2)(v_1^{ab})^2$, which varies between zero at Γ and $16(v_1^{ab})^2$ at *X*. The *c*'s can all be fitted at Γ giving the

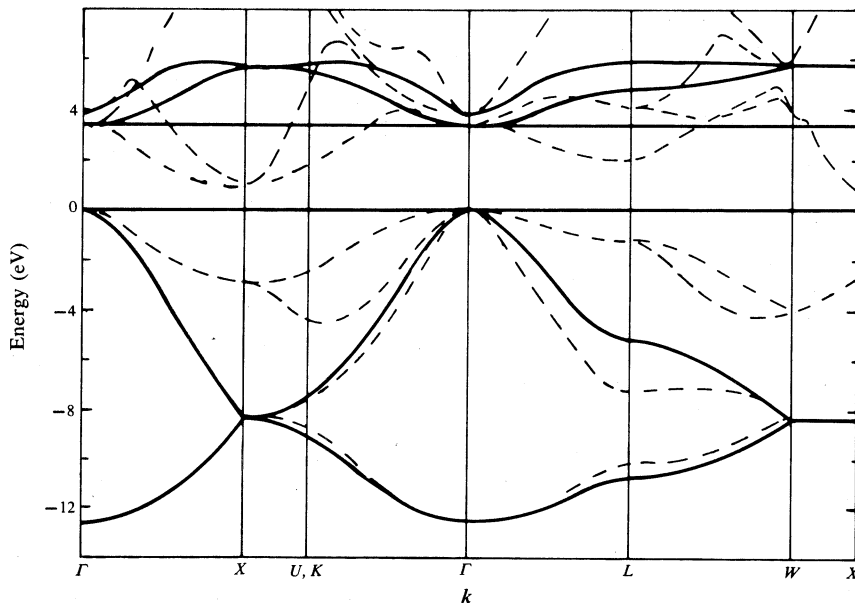


Fig. 5. Tight-binding band structure for silicon (solid curves), with all n.n. bond interactions included (i.e. with bonding-antibonding), compared with the pseudopotential results (dashed curves). The parameters are as given in Fig. 4, with the inclusion of $v_1^{ab} = -1.25$ eV.

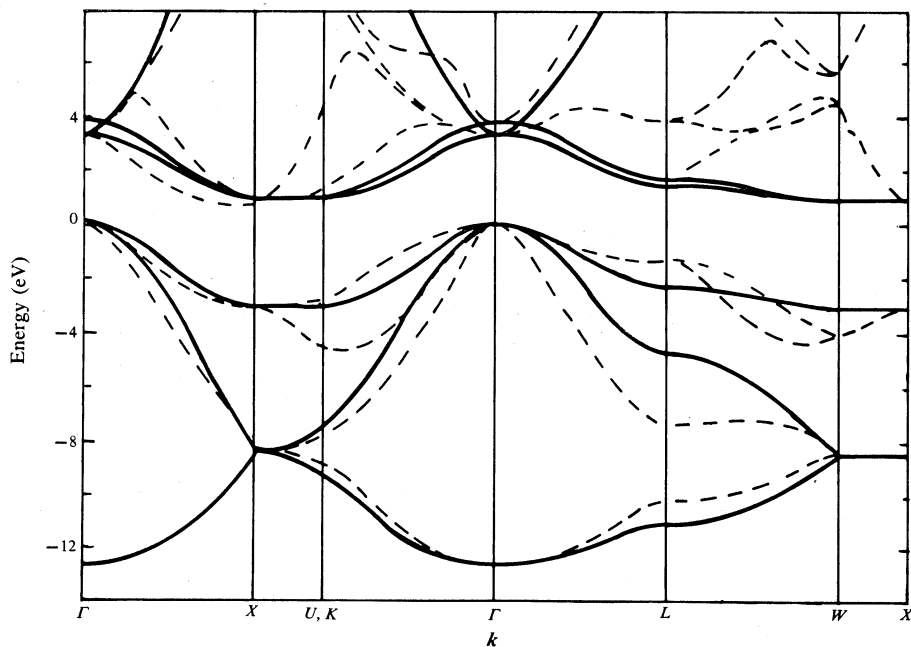


Fig. 6. Pure bonding and antibonding tight-binding bands (i.e. without bonding-antibonding interactions) for all central second n.n. bond interactions (solid curves), compared with the pseudopotential results for silicon (dashed curves). The parameters used are (in eV) $c_0^b = -8.39$, $c_1^b = -1.58$, $c_2^b = 0.13$, $c_0^{\pi b} = -3.03$, $c_2^{\pi b} = 0.19$, $c_0^a = 0.94$, $c_1^a = 0.06$, $c_2^a = 0.17$, $c_0^{\pi a} = 12.21$ and $c_2^{\pi a} = -0.55$.

same values as in Section 3*b*, leaving only v_1^{ab} to be found by fitting at X . However, it is not possible to fit simultaneously both conduction X_1^c and valence X_1^y sp bands; the bands shown in Fig. 5 have v_1^{ab} chosen to fit X_1^y , with the consequence that the energy for X_1^c is too high. The π bands remain flat.

Comparison with the pseudopotential results (dashed curves in Fig. 5) shows that the lower two valence bands are a very good fit along ΓX , with a poorer fit in other directions and in particular near L where the second band is too high. The π bands are quite inadequate, while the conduction sp bands behave in a fashion almost opposite to that of the pseudopotential bands. Thus, while adding the bonding–antibonding interaction has improved the fit considerably, especially in steepening the second valence band, the model is still far from a good representation of the bands even along ΓX .

(*d*) Second Nearest-neighbour Interactions

The pure bonding and antibonding bands including second n.n. interactions are as given in equation (50). The new term ε^2 introduces asymmetry into the mean values of the bands, as shown in Fig. 6. The parameters have been chosen to fit all energies at Γ and X . We see that the lower two valence bands are still somewhat rounded in shape and generally are a poorer representation of the pseudopotential bands throughout the zone than for the n.n. model including bonding–antibonding interactions (Fig. 5). However, the two sp conduction bands now behave in a manner more similar to the pseudopotential results, although they are too close together. The most important point to note is that the model π bands are no longer flat. The model valence π band along ΓX is slightly higher and more rounded than the pseudopotential band, but is a reasonable fit, while the dispersion ΓL is greater than given by the pseudopotential calculation. The degeneracy of the pseudopotential π bands is lifted along ΓKX and LW , and there is considerable dispersion along WX . These features are not accounted for in the central model. In fact since $\varepsilon = 0$ along WX , all the central bands are flat in this direction.

(*e*) Complete Central Solution

Finally, we include the bonding–antibonding interactions for both first and second n.n. bonds to give the complete solution, equations (40), (44) and (49). In this case there is insufficient information at Γ and X to fit all the parameters. As shown in the Appendix, all but three of the parameters are uniquely determined at these points, with the remaining three being determined by fitting at $2\pi(0.5, 0, 0)/a$. The resulting band structure is shown in Fig. 7.

The lowest (s-like) valence band is now an excellent fit throughout the zone, as is the second valence band along ΓX . The shape of this second band is improved in other directions although it remains too high along ΓL and LW . The π bands are unchanged, since we ignored any bonding–antibonding interactions for these states. The separation between the sp conduction bands has increased, but the fit to the pseudopotential bands is good along ΓX only. Note, however, that the model second sp conduction band is in excellent agreement with the lowest pseudopotential conduction band along most of ΓK and UX (i.e. apart from near Γ), and that both model bands have the same behaviour as the pseudopotential bands along ΓL , but shifted to lower energies. Both these features are relatively insensitive to the values of the fitting parameters.

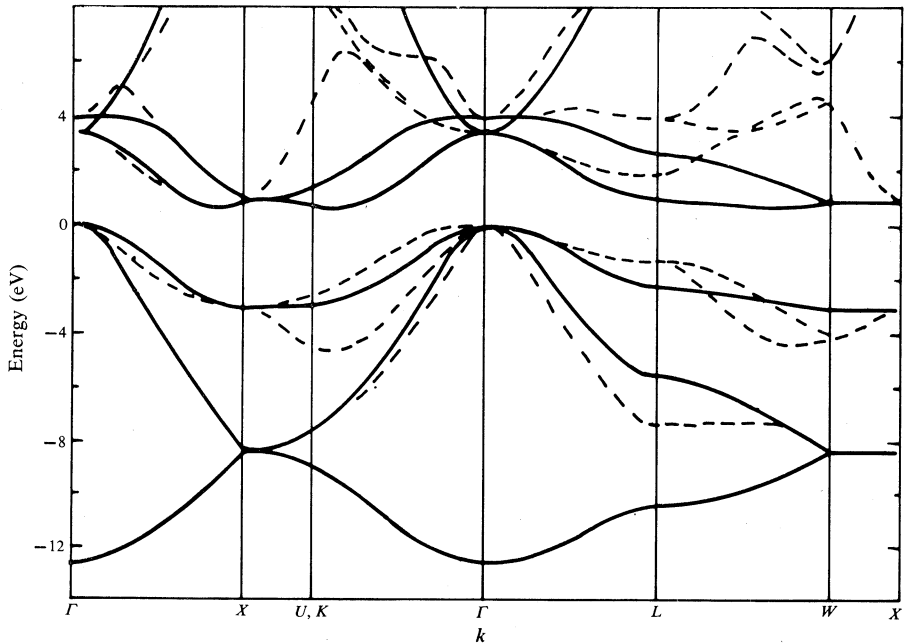


Fig. 7. Central model solution (including bonding-antibonding interactions) for all second n.n. bond interactions (solid curves), compared with the pseudopotential results for silicon (dashed curves). The parameters used for the central solution are given in Table 2.

Table 2. Values (in eV) for the various parameter sets for silicon

Values are obtained by fitting the central model to pseudopotential bands at Γ and X (see the Appendix)

| | Empirical | | Bonds | | | | sp ³ orbitals | | | | |
|-----------------|-----------|---------------|-------|---------------|-------|---------------------------------|--------------------------|---------------|-------|------------------|-------|
| c_0^b | -7.18 | c_0^a | -0.28 | v_0^b | -4.99 | v_0^a | 4.99 | V_1 | -2.20 | V_7 | -0.64 |
| c_1^b | -1.58 | c_1^a | 0.06 | v_1^b | -1.31 | v_1^a | -1.53 | V_2 | -4.99 | V_8 | -0.03 |
| c_2^b | 0.05 | c_2^a | 0.24 | v_{2c}^b | -0.14 | v_{2c}^a | 0.80 | V_3 | 0.11 | V_9 | 0.33 |
| $c_{0^b}^{\pi}$ | -3.03 | $c_0^{\pi a}$ | 12.21 | v_{2t}^b | 0.25 | v_{2t}^a | -0.31 | V_4+V_{12} | 0.55 | $3V_{11}+V_{12}$ | -1.72 |
| $c_{2^b}^{\pi}$ | 0.19 | $c_2^{\pi a}$ | -0.55 | $v_1^{\pi b}$ | -0.78 | $v_{2t}^{\pi a}+v_{2c}^{\pi a}$ | 0.20 | $3V_5-V_{12}$ | -1.07 | | |

Comparison of Figs 5-7 shows that the complete solution is necessary in order to obtain a satisfactory representation of the bands along ΓX . The only real discrepancy with the fit is for the region of high dispersion of the A_2 conduction band near Γ . A better fit to this region can be obtained by increasing $v_{2t}^{ab}+3v_{2c}^{ab}$, but at the expense of the fit to other bands. Note, however, that the conduction band minimum along ΓX is well reproduced by the model, requiring only that $v_{2t}^{ab}+3v_{2c}^{ab}$ be positive.

The terms involved in the complete second n.n. model are also thought to be sufficient to describe adequately the contributions of central interactions. The inclusion of third and more distant neighbour interactions will introduce higher order terms in ϵ , which may lead to a slightly improved fit, but they are unlikely to alter the bands in any substantial manner. Support for this view comes from the excellent fit to all the bands along ΓX , and of the lowest valence band throughout the zone. The agreement of the dispersion of these bands with the k dependence of the

second n.n. model is so good that there is no evidence for the need to include higher order terms. Further support comes from the observation that the values of the sp^3 interaction parameters, as derived from the fitted parameters (Table 2), are physically reasonable. This is an important result, for if it were not the case it too would indicate the need to consider higher order terms. This is not to say that inclusion of such terms would not alter the sp^3 values; rather, it means that the values obtained from the second n.n. bond model are quite adequate, so that any alterations are likely to be small.

The differences between the model and pseudopotential bands in Fig. 7 can therefore be attributed to non-central interactions. Thus all bands, apart from the lowest valence band, are affected by non-central interactions. In particular, the second lowest valence band is lowered and flattened along ΓL and LW , and the degenerate π -valence bands are lifted along ΓL . This upward shift is very similar to the shift for the lowest two conduction bands, so that the gap along ΓL is approximately the same with and without the non-central contribution, i.e. the gap appears to be determined predominantly by the central interactions. The degeneracy of the π bands is lifted by the non-central interactions along ΓK , UX and LW ; the conduction bands also demonstrate a pronounced non-central effect in these directions.

4. Conclusions

We have derived an analytical solution for the tight-binding sp^3 band structure of silicon, in the approximation that only central interactions are considered. In order to obtain a reasonable fit to the pseudopotential bands, especially along ΓX , we found it necessary and sufficient to include all interactions between first and second n.n. bonds. With n.n. interactions only we found that the bonding and antibonding sub-bands were merely scaled replicas of the s-band structure, together with flat π bands. Addition of second n.n. interactions introduced some dispersion into the π bands, and some asymmetry into the sp bands, so that all bands could be fitted at both Γ and X . However, the shape of the bands along ΓX can only be obtained accurately when the bonding-antibonding interactions are included.

The solutions obtained here are an extension of those obtained by Weaire and coworkers (see e.g. Weaire and Thorpe 1973), from a much simpler interaction model. As in the simpler model, all the k dependence of the present solution is contained in the function $\epsilon(k)$, which is determined entirely by the topology of the structure. Thus, the earlier results obtained by Weaire and Thorpe (1971), which depend only on the relationship between the k dependence of the sp^3 bands and $\epsilon(k)$, remain valid for this extended model. Indeed, they are now seen to be common to all central approximation models. Of particular interest is the one-to-one relationship between electronic and vibrational spectra in these models (Weaire and Alben 1972). A similar transformation can be applied to the present model to give the second n.n. central field solution for the vibrational states.

The analytical nature of the solution allows many possibilities for future work. For example, we could undertake a study of the general properties of fourfold coordinated materials as has been done with the bond-orbital model (Harrison and Ciraci 1974; Harrison 1981). Not only can the band energies be calculated rapidly and simply with the aid of no more than a pocket calculator, but fitting the ΓX solution may provide the best values of the sp^3 parameters for more complete calculations. However, it is probably in the study of topological changes that these models will

find the greatest application, mainly because of the tremendous simplification that results from having to study only $\epsilon(\mathbf{k})$ for the structure and not a full sp^3 basis. In this respect we note that the s-band structures [or $\epsilon(\mathbf{k})$, they are essentially the same thing] of all close-packed polytypes are equivalent under a one-to-one \mathbf{k} -space transformation which is valid throughout the zone (Betteridge 1981a, 1981b). Thus, for example, we can easily show that the central contribution to the sp^3 densities of states for all these structures is identical.

References

- Betteridge, G. P. (1973). Ph.D. Thesis, Univ. of Cambridge.
 Betteridge, G. P. (1974). *J. Phys. C* **7**, L446.
 Betteridge, G. P. (1981a). *Phys. Status Solidi (b)* **107**, 791.
 Betteridge, G. P. (1981b). *Phys. Status Solidi (b)* **108**, 245.
 Chadi, D. J., and Cohen, M. L. (1975). *Phys. Status Solidi (b)* **68**, 405.
 Cohen, M. L., and Bergstresser, T. K. (1966). *Phys. Rev.* **141**, 789.
 Harrison, W. A. (1981). *Phys. Rev. B* **23**, 5230.
 Harrison, W. A., and Ciraci, S. (1974). *Phys. Rev. B* **70**, 1516.
 Heine, V. (1971). *J. Phys. C* **5**, L221.
 Huang, I. L., and Dy, K. S. (1974). *Phys. Rev. B* **9**, 5316.
 Hulin, M. (1972). *Phys. Status Solidi (b)* **52**, 119.
 Joannopoulos, J. D., and Cohen, M. L. (1976). In 'Solid State Physics', Vol. 31 (Eds H. Ehrenreich *et al.*), p. 89 (Academic: New York).
 Lohez, D., Lannoo, M., and Allan, G. (1981). *Solid State Commun.* **39**, 573.
 Schwartz, L., and Ehrenreich, H. (1972). *Phys. Rev. B* **6**, 4088.
 Slater, J. C., and Koster, G. F. (1954). *Phys. Rev.* **94**, 1498.
 Straley, J. P. (1972). *Phys. Rev. B* **6**, 4086.
 Streitwolf, H. W. (1974). *Phys. Status Solidi (b)* **63**, 529.
 Tanaka, K., and Tsu, R. (1981). *Phys. Rev. B* **24**, 2038.
 Thorpe, M. F., and Weaire, D. (1971). *Phys. Rev. B* **4**, 3518.
 Weaire, D. (1971). *Phys. Rev. Lett.* **26**, 1541.
 Weaire, D., and Alben, R. (1972). *Phys. Rev. Lett.* **29**, 1505.
 Weaire, D., and Thorpe, M. F. (1971). *Phys. Rev. B* **4**, 2508.
 Weaire, D., and Thorpe, M. F. (1973). In 'Computational Methods for Large Molecules and Localised States in Solids' (Eds F. Herman *et al.*), p. 295 (Plenum: New York).

Table 3. Pseudopotential results for silicon (in eV)

The zero of energy has been set at $E(\Gamma_{25'})$. The pseudopotential results were calculated with $V(|G^2| = 3) = -0.105$ a.u., $V(8) = 0.02$ a.u. and $V(11) = 0.04$ a.u. (Betteridge 1973). The degeneracies are given in parentheses

| Γ , $2\pi(0, 0, 0)/a$ | ΓX , $2\pi(\frac{1}{2}, 0, 0)/a$ | X , $2\pi(1, 0, 0)/a$ |
|------------------------------|------------------------------------------|-------------------------|
| Γ_1 -12.65 | A_1 -11.54 | X_1 -8.39(2) |
| $\Gamma_{25'}$ 0.00(3) | $A_{2'}$ -3.81 | X_4 -3.03(2) |
| Γ_{15} 3.39(3) | A_5 -2.01(2) | X_1 0.94(2) |
| $\Gamma_{2'}$ 3.85 | A_1 1.49 | X_3 12.21(2) |
| | $A_{2'}$ 3.51 | |
| | A_5 7.05(2) | |

Appendix

The tight-binding parameters are chosen by fitting the central solution to the energies at Γ and X , as calculated by the empirical pseudopotential method (Cohen and Bergstresser 1966). The values used here are shown in Table 3.

There is no bonding-antibonding interaction at Γ , since $\varepsilon^2 = 16$. Hence the pure bonding and antibonding solutions are eigenfunctions; Γ_1 corresponds to E_+^b , Γ_{25} to E_-^b , Γ_2 to E_+^a and Γ_{15} to E_-^a . Furthermore, we have

$$E_{\pm}^b(\Gamma) = c_0^b \pm 4c_1^b + 16c_2^b, \quad E_{\pm}^a(\Gamma) = c_0^a \pm 4c_1^a + 16c_2^a. \quad (\text{A1})$$

Nearest-neighbour Bonds Only

In this case there is no ε^2 term, so $c_2^b = c_2^a = 0$. The remaining four parameters are all fitted at Γ . The valence bandwidth (12.64 eV) is given by $-8c_1^b$ and the conduction bandwidth (0.46 eV) by $8c_1^a$. The c_0^b and c_0^a are given by the midpoints (at Γ) of the valence and conduction bands respectively. Thus, in the n.n. approximation

$$c_0^b = -6.32 \text{ eV}, \quad c_0^a = 3.62 \text{ eV}, \quad c_1^b = -1.58 \text{ eV}, \quad c_1^a = 0.06 \text{ eV}. \quad (\text{A2})$$

The π bands are given by $E(\Gamma_{25})$ and $E(\Gamma_{15})$, i.e.

$$E_{\pi}^b = c_0^{\pi b} = 0 \text{ eV}, \quad E_{\pi}^a = c_0^{\pi a} = 3.39 \text{ eV}. \quad (\text{A3})$$

Nearest-neighbour Bonding-Antibonding

This term has no effect at Γ , or on the π bands, so that the c 's as given in equations (A2) and (A3) are unaltered. The extra term involves v_1^{ab} and is used to fit the energies at X ($\varepsilon = 0$). Thus, we have

$$E(X) = \frac{1}{2}(c_0^b + c_0^a) \pm \left\{ \frac{1}{2}(c_0^b - c_0^a)^2 + 16(v_1^{ab})^2 \right\}^{\frac{1}{2}}. \quad (\text{A4})$$

With the c_0 fixed at Γ , it is possible to choose v_1^{ab} to fit either X_1^b or X_1^a (or, indeed, their separation) but not both simultaneously. We choose to fit X_1^b , for which

$$v_1^{ab} = -1.25 \text{ eV}. \quad (\text{A5})$$

Second Nearest Neighbours

We now consider the complete expressions at Γ as in equations (A1). The bandwidths are still given by the c_1 only, but the midpoints are now given by (all energies in eV)

$$c_0^b + 16c_2^b = -6.32, \quad c_0^a + 16c_2^a = 3.62. \quad (\text{A6})$$

However, we can now obtain c_0^b and c_0^a from the energies at X [equation (A4) with $v_1^{ab} = 0$], so that

$$c_0^b = -8.39, \quad c_0^a = 0.94, \quad (\text{A7})$$

and therefore

$$c_2^b = 0.13, \quad c_2^a = 0.17. \quad (\text{A8})$$

The π bands can also be fitted at Γ and X , giving (in eV)

$$\begin{aligned} c_0^{\pi b} + 16c_2^{\pi b} = E(\Gamma_{25}) = 0, & \quad c_0^{\pi b} = E(X_4) = -3.03, \\ c_0^{\pi a} + 16c_2^{\pi a} = E(\Gamma_{15}) = 3.39, & \quad c_0^{\pi a} = E(X_3) = 12.21, \end{aligned}$$

that is,

$$c_0^{\pi b} = -3.03, \quad c_0^{\pi a} = 12.21, \quad c_2^{\pi b} = 0.19, \quad c_2^{\pi a} = -0.55. \quad (\text{A9})$$

Complete Solution

The situation at Γ is as above, so that equations (A6) still hold, and coefficients of the π bands are as in equations (A9). The difference now is that the c_0 can no longer be determined uniquely at X ; we must use equation (A4) with v_1^{ab} replaced by V_{\pm}^{ab} , as in equation (49). Thus the midpoint at X gives

$$c_0^b + c_0^a = -7.45. \quad (\text{A10})$$

Combined with equations (A6) we have

$$c_2^b + c_2^a = 0.30. \quad (\text{A11})$$

Until now we have treated the c 's as independent parameters. However, they are related to one another through the sp^3 interactions, as given in Table 1. We now use these relationships to assist with the fitting. In particular, we note that

$$c_2^b + c_2^a = \frac{1}{2}(v_{2c}^b + v_{2t}^b + v_{2c}^a + v_{2c}^b) = V_8 + V_9, \quad (\text{A12a})$$

$$c_2^{\pi b} + c_2^{\pi a} = \frac{1}{2}(v_{2t}^b + v_{2c}^b + v_{2t}^a + v_{2c}^a) = V_8 - V_9. \quad (\text{A12b})$$

Using values from equations (A9) and (A11), we have (again in eV)

$$V_8 = -0.03, \quad V_9 = +0.33, \quad (\text{A13})$$

and also

$$c_1^b + c_1^a = V_1 + V_7 + 4V_9 = -1.52,$$

and therefore

$$V_1 + V_7 = -2.84. \quad (\text{A14})$$

An adjustable parameter E_0 must be added to the constant term to give the (arbitrary) zero of energy, in this case $E(\Gamma_{25'}) = 0$. Hence, we get

$$c_0^b + c_0^a = 2E_0 + 2(V_1 + V_7) - 4V_8 - 8V_9 = -7.45,$$

so that

$$E_0 = 0.37. \quad (\text{A15})$$

The π bands also give

$$\begin{aligned} c_2^{\pi b} - c_2^{\pi a} &= \frac{1}{2}(v_{2t}^b - v_{2c}^b - v_{2t}^a + v_{2c}^a) \\ &= \frac{1}{2}(V_4 - V_5 - V_{11} + V_{12}) = 0.74, \end{aligned}$$

that is,

$$V_4 - V_5 - V_{11} + V_{12} = 1.48. \quad (\text{A16})$$

This is as far as one can go at Γ and X alone. There are still three parameters to be determined; denoting these by x , y and z , they are

$$x = c_2^b - c_2^a = \frac{1}{2}(V_4 + V_5 + V_{11} + V_{12}), \quad (\text{A17a})$$

$$y = v_1^{ab} = \frac{1}{2}(V_1 - V_7), \quad (\text{A17b})$$

$$z = \frac{1}{6}(v_{2t}^{ab} + 3v_{2c}^{ab}) = \frac{1}{12}(V_4 + 3V_5 - 3V_{11} - V_{12}). \quad (\text{A17c})$$

These parameters can be obtained from the sp splitting at X and $2\pi(0.5, 0, 0)/a$ (where $\varepsilon^2 = 8$):

$$(-4.97 - 8x)^2 + 16y^2 = 21.72, \quad (\text{A18a})$$

$$(-2.82 - 4x)^2 + 8(y - 2.83z)^2 = 13.39, \quad (\text{A18b})$$

$$(-7.12 - 4x)^2 + 8(y + 2.83z)^2 = 42.49. \quad (\text{A18c})$$

These are satisfied simultaneously by

$$x = -0.19 \text{ eV}, \quad y = -0.78 \text{ eV}, \quad z = 0.10 \text{ eV}. \quad (\text{A19})$$

Substituting into equations (A17), (A14) and (A16), we find (in eV)

$$V_1 = -2.20, \quad V_7 = -0.64, \quad V_4 + V_{12} = 0.55, \quad V_5 + V_{11} = -0.93, \quad (\text{A20})$$

and also

$$c_1^b - c_1^a = v_1^b + 2v_{2c}^b - v_1^a - 2v_{2c}^a = 2V_3 + 2V_5 + 2V_{11}.$$

and therefore

$$V_3 = 0.11. \quad (\text{A21})$$

Finally, we have

$$\begin{aligned} c_0^b - c_0^a &= v_0^b - v_0^a + 2(v_1^b - v_1^a) - 4(v_{2c}^b - v_{2c}^a) - 2(v_{2t}^b - v_{2t}^a) \\ &= 2V_2 + 4V_3 - 4V_5 - 4V_{11} - 2V_4 - 2V_{12}, \end{aligned}$$

so that

$$V_2 = -4.99. \quad (\text{A22})$$

Using these values for the V 's we can obtain all the v 's and c 's by substitution. These final results are presented in Table 2 (see Section 3e).

We note that another solution to equations (A18) is

$$x = -1.15 \text{ eV}, \quad y = -0.05 \text{ eV}, \quad z = -0.58 \text{ eV}. \quad (\text{A23})$$

The band structure obtained using this solution is essentially the same as that obtained from equations (A19). However, when expressed in terms of the sp^3 V interactions this second solution (A23) gives unrealistic values, and has therefore been discarded.